nature physics

SUPPLEMENTARY INFORMATION

DOI: 10.1038/NPHYS3416

# Itinerant density wave instabilities at classical and quantum critical points

Yejun Feng[1, 2], Jasper van Wezel[3], Jiyang Wang[2], Felix Flicker[4], D. M. Silevitch[2], P. B. Littlewood[2, 5], T. F. Rosenbaum[2, 6]

[1]The Advanced Photon Source, Argonne National Laboratory, Argonne, Illinois 60439, USA
[2]The James Franck Institute and Department of Physics, The University of Chicago, Chicago, Illinois 60637, USA
[3]Institute for Theoretical Physics, University of Amsterdam, 1090 GL Amsterdam, The Netherlands
[4]H. H. Wills Physics Laboratory, University of Bristol, Bristol BS8 1TL, UK
[5]Physical Sciences and Engineering, Argonne National Laboratory, Argonne, Illinois 60439, USA
[6]Division of Physics, Mathematics, and Astronomy, California Institute of Technology, Pasadena, California 91125, USA

## NUMERICAL EMULATION OF $Q(T, P)$ EVOLUTION IN $NbSe_2$

### a. Construction of CDW phase distortion using McMillan's discommensuration model

A distortion $\Delta\phi(x)$ of the CDW phase $\phi(x)$ from a purely sinusoidal form, engages the lock-in term $f\psi^n \cos(n\phi - Gx)$ in Eq. 1 and results in the presence of higher harmonics of the primary wave. A growing phase distortion effectively interpolates between an incommensurate CDW at the $Q$-vector preferred by the full susceptibility and a commensurate CDW locked into the lattice [40]. Our diffraction results (Fig. 3b, 6c) provide the relative intensities but not the relative phases between harmonics, and hence it is not possible to experimentally reconstruct $\Delta\phi(x)$. To simulate $Q(T, P)$ as we show in Fig. 5, we use McMillan's discommensuration model [40] to construct a functional form of $\Delta\phi(x)$ for smooth and wide phase distortions. The CDW phase $\phi(x)$ is expressed using a limited number (i.e. two) of parameters:

$$\phi_{discomm}(x) = 2\pi\left(\tfrac{1}{3} + \alpha\left(q - \tfrac{1}{3}\right)\right)x - \tfrac{1}{3}\textstyle\sum_n \frac{\beta^n}{n}\sin(2\pi n(1-3q)\alpha x). \qquad \text{(S1)}$$

Here, $x$ and $q$ are written in units of the real and reciprocal and space lattice constants, respectively. With $\beta = 0$, Eq. S1 represents a perfectly sinusoidal wave, with a varying wave vector determined by $\alpha$. At $\alpha = 0$, the CDW is locked in at the commensurate wave vector of 1/3 r.l.u., while for $\alpha = 1$, the CDW propagates at the natural, incommensurate $q$ value preferred by the susceptibility, which equals the experimentally measured wave vector $Q(T_{DW}, P)$ (purple dashed line in Fig. 1a). For nonzero values of $\beta$, the perfect sinusoidal CDW is distorted, and $2\pi/3$ phase slips appear at spatial separations of



© 2015 Macmillan Publishers Limited. All rights reserved

DOI: 10.1038/NPHYS3416

$\xi_0 = \frac{1}{3\delta} = \frac{1}{[(1-3q)\alpha]}$. The parameter $\beta$ controls the width of these distortions. For $\beta = 1$, the phase slips are infinitely narrow, and the function $\phi(x)$ is a series of straight lines with slope $\frac{2\pi}{3}$ separated by sharp steps. For $\beta < 1$, the steps become smooth, and the phase distortions obtain a finite width.

**b. Determining parameters by minimization of free energy and global *Q*(*T, P*) behavior**

The free energy *F* (Eq. 1) can be minimized with respect to the parameters $\alpha$ and $\beta$ for any given set of coefficients *a*, *b*, *e*, *f*, and *q*. During the minimization, we approximate the amplitude of the CDW to be fixed by the first two terms in *F*, so that $\psi^2 = \frac{a}{2b}$, which is justified as long as $e, f << b$. The values of $\alpha$ and $\beta$ that minimize the spatially integrated free energy *F* thus are only a function of $\frac{f}{e}\psi$ and *q*. In these numerical minimizations, we retained 200 powers of $\beta$ in the functional form of Eq. (S1), and employed a real space grid of 250,000 sites, covering 5,000 atoms.

In the free energy minimization process described above, we notice $\alpha$ and $\beta$ are smoothly varying as a function of $\frac{f}{e}\psi$ and q. To reduce computation time, the free energy minimization was performed at selected values of $\frac{f}{e}\psi$ and q, and smooth interpolating functions were used to generate $\alpha$ and $\beta$ values in successive calculations.

The constraints imposed on the parameters *a*, *b*, *e*, *f*, and *q* in the free energy *F* (Eq. 1) over the pressure-temperature space are discussed in the main text, based on physical considerations. As mentioned, there are consequently only two parameters left to determine *Q*(*T, P*). They are related to the competition between the fourth and fifth terms in Eq. 1, with the coefficient *f* approximated as $f(P) = f_0 + f_1 P$. The first parameter is the ratio $\frac{f_0}{e}$, which sets the evolution of the phase distortions at ambient pressure, and hence *Q*(*T*, *P*=0). The coefficient $f_1$ dictates the evolution under pressure. We chose the first parameter so the range of simulated *Q*(*T, P*=0) equals that of the experimental results. Subsequently, we chose the value of $f_1$ such that *Q*(*T*=0*, P*) reaches the turning point of its non-monotonic evolution at about 2.3 GPa, similar to the experimental results at 3.5 K (Fig. 1a). The resulting simulated *Q*(*T, P*) is shown in Fig. 5.

**c. Characteristics of simulated CDW states**

Having optimized the temperature and pressure dependence of *Q*(*T*, *P*) we now discuss a few characteristics of the simulated CDW states, which follow from the corresponding temperature and pressure dependencies of the parameters $\alpha$ and $\beta$.

The simulated *Q*(*T*, *P*=0) is presented in Fig. S1. Although the shape and curvature are different from that seen in the experimental data (Fig. 2a), the overall monotonically changing trend is preserved. The difference between simulation and



© 2015 Macmillan Publishers Limited. All rights reserved

experiment is due to the combination of restricting the functional form of $\phi(x)$ in Eq. S1, and the linear temperature dependence of the coefficient $a$.

The real space charge modulation $\psi \cos(\phi(x))$ can be Fourier transformed (FT) to directly simulate the experimentally observed diffraction pattern, as the intensity $I$ is proportional to the square of the FT amplitude. Two representative spectra at ambient pressure are presented in Fig. S2. To increase the precision with which we can determine the peak heights, we oversampled the FT. This allows us to get a dense set of data points around the incommensurate peak positions, but it also results in ringing near the tails of all peaks, as a consequence of the Nyquist effect. Nevertheless, higher harmonics in Fourier space are observed as expected from the simulated phase distortion of Eq. S1. In Fig. S3, we plot intensity ratios of four strongest harmonics to the primary wave as a function of temperature at ambient pressure. We notice the intensity ratio of second harmonic to the primary peak reaches 0.037 at base temperature, in comparison to 0.012 of experimental results (Fig. 4 inset). Although the intensity of harmonics tends to drop with increasing distance from the main peak (see Fig. S3), the intensities of the fourth, fifth, seventh, and tenth harmonics lie above the experimental sensitivity limit of ~1 $10^{-4}$ (see Fig. 3 and Fig. 6c). The presence of these additional harmonics can be attributed to the restricted functional form imposed for $\phi(x)$ by Eq. S1. Nevertheless, the trend of the harmonic ratios as a function of temperature is qualitatively correct. The intensity ratios are the largest at base temperature, and monotonically disappear as the transition temperature is approached.

For CDW states under pressure, our experimentally measured primary CDW has a signal to noise ratio much less than 50:1 (Ref. [5], Fig. 6b), mostly due to an increased elastic scattering background from diamond anvils as a part of the high pressure sample environment. Thus it is insufficient to reveal higher harmonics. Nevertheless, simulation can provide qualitatively predictions of the higher harmonics behavior. As the simulated CDW becomes commensurate for a finite pressure range at base temperature (Fig. 5), the harmonic ratios cannot be unambiguously defined. Instead, we plot the harmonic ratios at $T = 9.4$ K, a temperature which is about 1/3 of $T_c$ at ambient pressure (Fig. S4). We notice that the harmonic ratio is also non-monotonic. The simulation and experiment agree that the CDW is always a perfect sine wave without any phase distortions or higher harmonics at $T = T_{CDW}(P)$.



© 2015 Macmillan Publishers Limited. All rights reserved

DOI: 10.1038/NPHYS3416

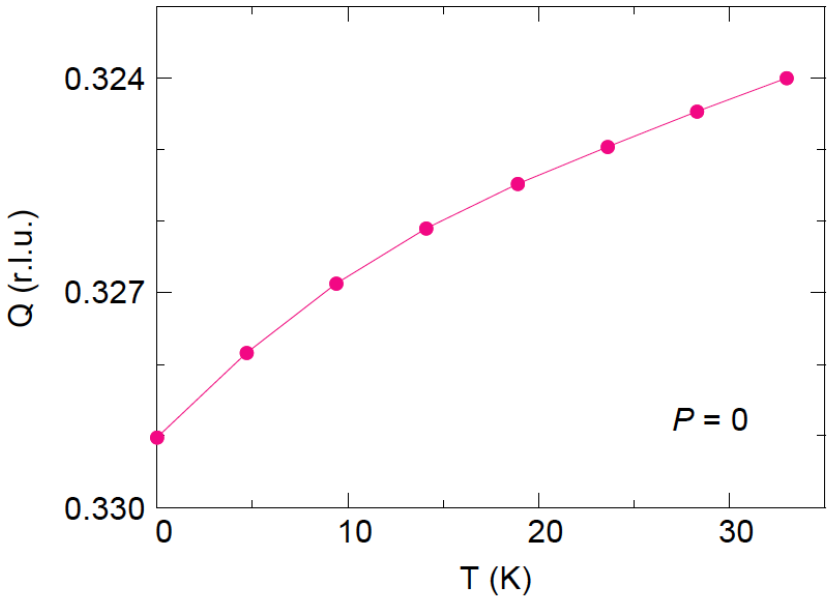


**Fig. S1:** Simulated $Q(T)$ evolution of $NbSe_2$ at ambient pressure.



© 2015 Macmillan Publishers Limited. All rights reserved

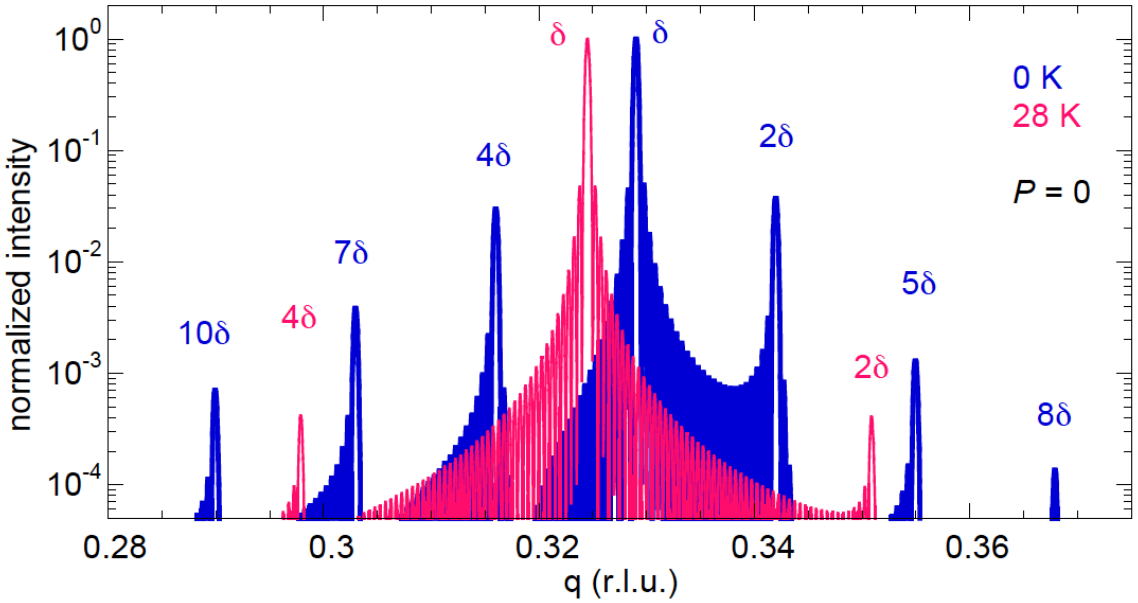


**Fig. S2:** Simulated CDW diffraction profiles Fourier transformed from simulated CDW states at 0 K and 28 K. They represent $\beta$ values of 0.54 and 0.054 respectively.



© 2015 Macmillan Publishers Limited. All rights reserved

DOI: 10.1038/NPHYS3416

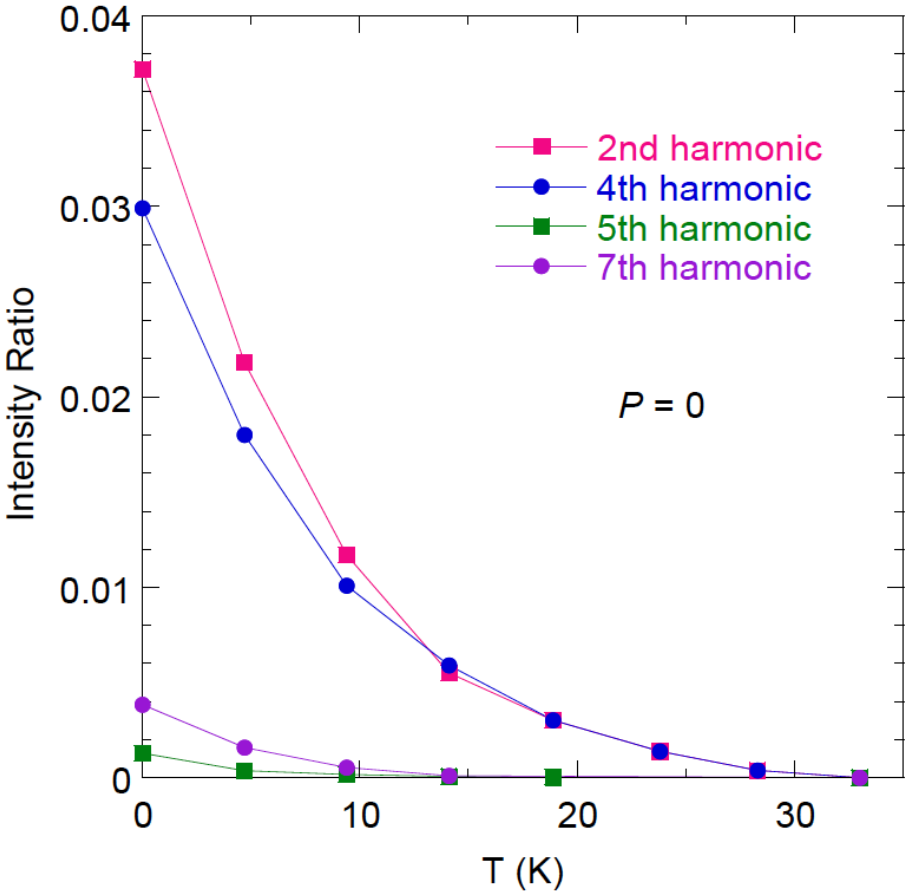


**Fig. S3:** Temperature evolutions of intensity ratio of higher harmonics to the primary CDW.



© 2015 Macmillan Publishers Limited. All rights reserved

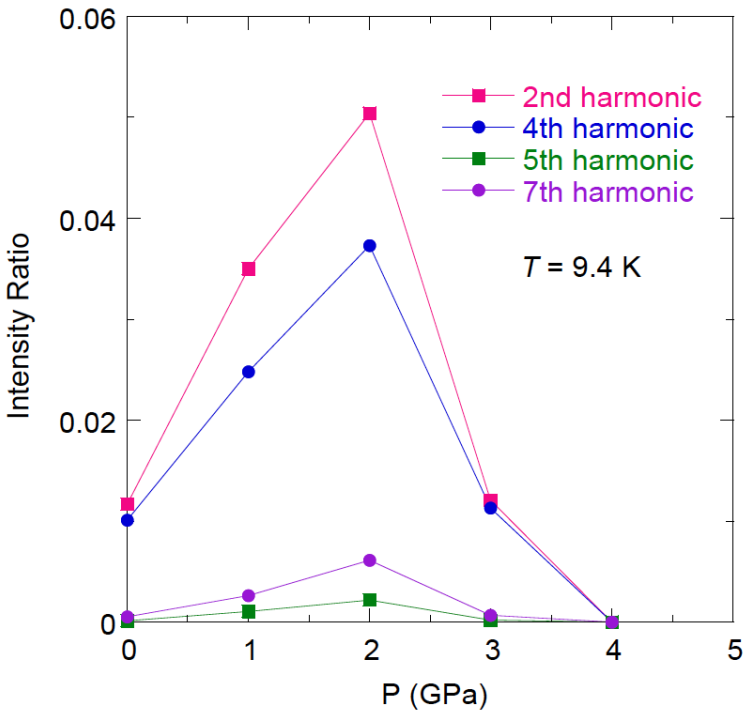


**Fig. S4:** Pressure evolutions of intensity ratio of higher harmonics to the primary CDW, taken at 9.4K.



© 2015 Macmillan Publishers Limited. All rights reserved